THE JOURNAL OF PHYSICAL CHEMISTRY LETTERS
A JOURNAL OF THE AMERICAN CHEMICAL SOCIETY

pubs.acs.org/JPCL

Letter

Pioglitazone Inhibits Metal Cluster Transfer of mitoNEET by Stabilizing the Labile Fe−N Bond Revealed at Single-Bond Level

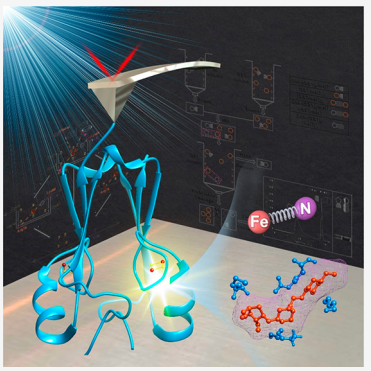
Guobin Song, Fang Tian, Huaxing Liu, Guoqiang Li, and Peng Zheng*

Cite This: *J. Phys. Chem. Lett.* 2021, 12, 3860−3867

Read Online

ACCESS | Metrics & More | Article Recommendations | Supporting Information

ABSTRACT: Outer mitochondrial membrane protein mitoNEET (mNT) is a target of the type 2 diabetes drug pioglitazone. It contains a labile $Fe_2S_2(His)_1(Cys)_3$ metal cluster with a single Fe−N(His87) coordinating bond and can transfer its cluster to acceptor proteins. Previous ensemble studies showed that pioglitazone's binding inhibited the transfer by stabilizing the cluster, and histidine 87 may be the key mediator. Here we used atomic force microscopy-based single-molecule force spectroscopy (AFM-SMFS) to study the unfolding process of mNT dimer in the absence and presence of pioglitazone, which can distinguish the binding effect for different regions of a protein. By developing a two-step strategy using different mNT monomers with respective purification tags, we solve the problem that the classic polyprotein formation disables the mNT to dimerize. As a result, a polyprotein including a stable, naturally noncovalently bound mNT homodimer is obtained, which is required for reliable AFM measurement and pioglitazone binding. Then, the dissociation rate (k_{off}) of the metal cluster was measured, showing a 10-fold decrease upon pioglitazone binding, while the other parts decreased only 3-fold, verifying that pioglitazone mainly stabilizes the cluster. Moreover, when the Fe(III)−N(His87) bond was ruptured, this effect for the remaining $Fe_2S_2(Cys)_3$ intermediate largely disappeared. Consequently, AFM results revealed that pioglitazone inhibited the metal cluster transfer of mNT by stabilizing the labile Fe(III)−N(His87) bond. In addition, an alternative method to build a natural, noncovalently bound protein dimer or complex for reliable single-molecule measurement was developed.



Iron−sulfur protein is an ancient protein family essential for almost all kingdoms of life. Because of the FeS cluster, it plays critical roles in many biological processes, such as electron transport and catalysis.[1−3] Recently, a novel Fe−S protein on the outer mitochondrial membrane mitoNEET (mNT) was found with a labile $Fe_2S_2(His)_1(Cys)_3$ iron−sulfur cluster, which can transfer the cluster to acceptor proteins like apo-ferredoxin. Moreover, mNT binds to the type II diabetes drug pioglitazone, being the first discovered FeS protein of a drug target.[4,5] Previous ensemble studies showed that the pioglitazone binding stabilized the iron−sulfur cluster; inhibited cluster transfer; and may alleviate iron overload in mitochondria, in which the cluster-coordinating residue His87 was the essential mediator.[6−8] Mutating this histidine to cysteine disables mNT to transfer its cluster to apo-ferredoxin shown by biochemistry assay.[4] Also, our previous single-molecule AFM work showed the labile Fe(III)−N(His87) bond enabled the multiple rupture pathways of the metal cluster in mNT monomer and may be responsible for cluster transfer.[9] Thus, here we used AFM to study the relationship between pioglitazone binding and the Fe(III)−N(His87) bond to further understand the effect at the single-bond level.

Human mNT is a 108 amino acids (aa)-length, integral protein of the mitochondrial outer membrane with a soluble part from residues 33 to 108, which presents as a stable, naturally occurring homodimer. Each monomer folds into two parts: a 2Fe2S cluster-binding motif (residues 72−87) and a three-strand β-sheet motif (residues 56−61, 68−71, and 98−104). The cluster is coordinated by one imidazole nitrogen (His87) and three sulfurs (Cys72, Cys74, and Cys83) (Figure 1A).[10] Photoaffinity experiments showed that the pioglitazone bound to mitoNEET in vitro.[7] Pioglitazone is a thiazolidinedione derivative functioning as potent insulin sensitizers for the treatment of type II diabetes. Ensemble studies suggested that pioglitazone inhibits the transfer process of the iron−sulfur cluster by stabilizing the metal cluster. In addition, the binding site has not been identified. Previous docking studies by other groups showed the two most possible binding sites: site 1 composed of Lys89, Lys42, Arg76, and Met44 and site 2 composed of Arg76 and Glu93.[11] These results provide valuable insight into the binding site based on the direct interaction between pioglitazone and the protein. Nevertheless, it lacks the effect for the metal cluster, and further evidence is necessary.

Received: December 30, 2020
Accepted: April 12, 2021
Published: April 15, 2021



Downloaded via NANJING UNIV on July 12, 2021 at 11:27:07 (UTC).
See https://pubs.acs.org/sharingguidelines for options on how to legitimately share published articles.

ACS Publications

© 2021 American Chemical Society

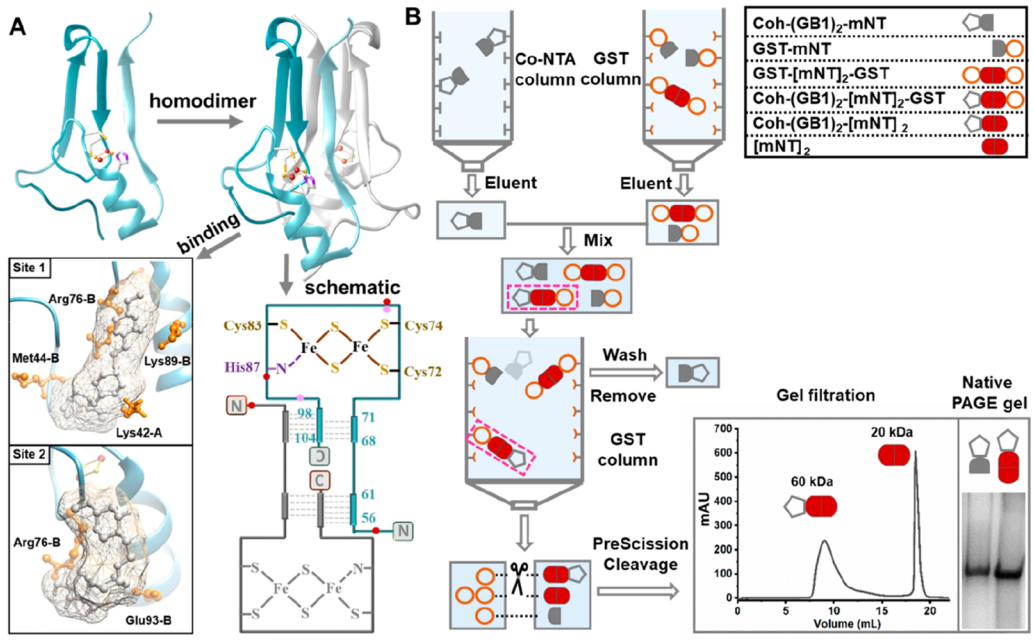


Figure 1. (A) Three-dimensional structure and simplified schematic of mNT homodimer. The 2Fe2S cluster is coordinated by a unique single histidine (87) and three cysteines (72, 74, and 83). Two possible pioglitazone binding sites on the mNT dimer by docking experiment are shown.[11] Lys89 in site 1 is the closest residue to His87. (B) The polyprotein with mNT dimer, Coh-$(GB1)_2$-$[mNT]_2$, is obtained by mixing two different monomers $(His)_6$-Coh-$(GB1)_2$-mNT and GST-mNT. His-tag and GST-tag are used for their purification, respectively. The protein is verified and/or purified by gel filtration using FPLC and native PAGE gel after GST-tag cleavage (graphs in the bottom right).

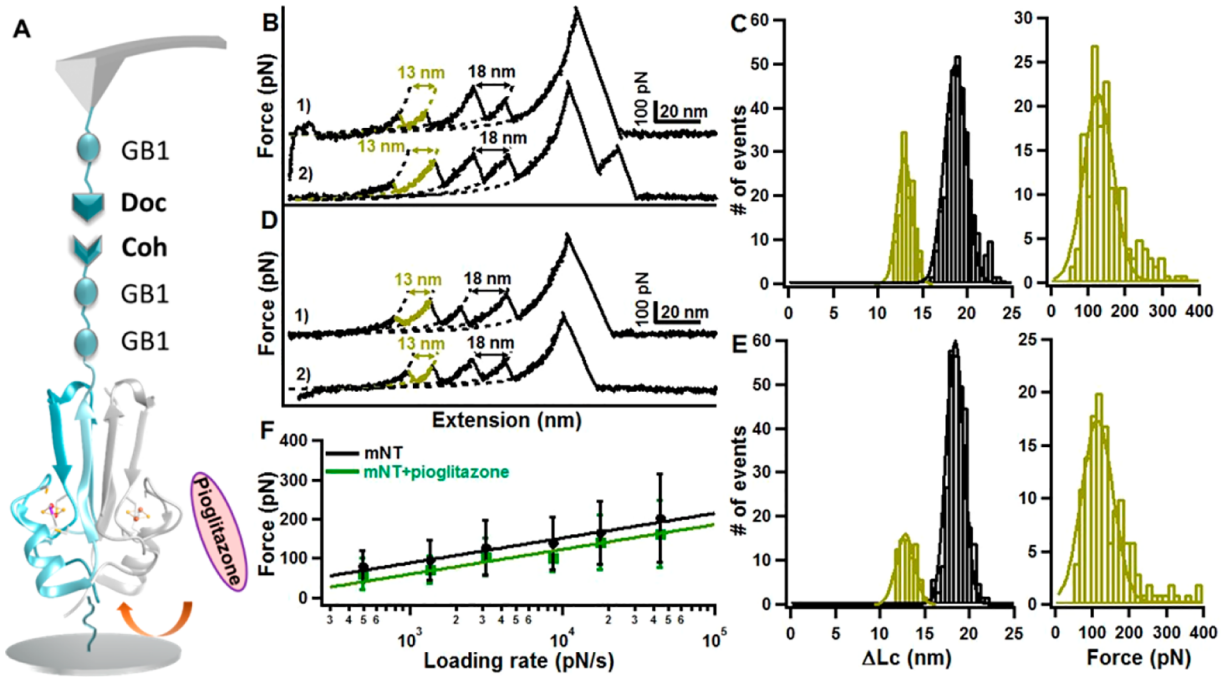


Figure 2. AFM unfolding results of mNT with or without pioglitazone binding. (A) Single-molecule AFM setup shows that the polyprotein Coh-$(GB1)_2$-$[mNT]_2$ is recognized by the GB1-Doc on the tip through the specific [Doc-Coh] interaction. (B) Representative force−extension curves of mNT show the 13 nm peak is from the one-step unfolding of the mNT (yellow). (C) Histogram of ΔLc (left) and unfolding force (right, for 13 nm peak) of mNT. (D) Force−extension curves show the unfolding of pioglitazone-bound mNT (yellow). (E) ΔLc and unfolding force histogram of pioglitazone-bound mNT. (F) Rupture forces of mNT (black circle) and mNT−pioglitazone complex (green square) are measured at different pulling speeds. The data points are fitted by the Bell−Evans model to obtain the kinetic parameters.

Atomic force microscopy (AFM), along with optical and magnetic tweezers, can be used as single-molecule force spectroscopy (SMFS), which manipulates single molecules mechanically, induces the break of intramolecular or intermolecular interactions, and captures the transient state.[12−17] It has been widely used to study protein (un)folding,[18−24] protein−ligand (protein) interaction, and chemical bonding,[25−32] because of its high force range and excellent length resolution. Thus, we choose AFM-SMFS,

https://doi.org/10.1021/acs.jpclett.0c03852
J. Phys. Chem. Lett. 2021, 12, 3860−3867

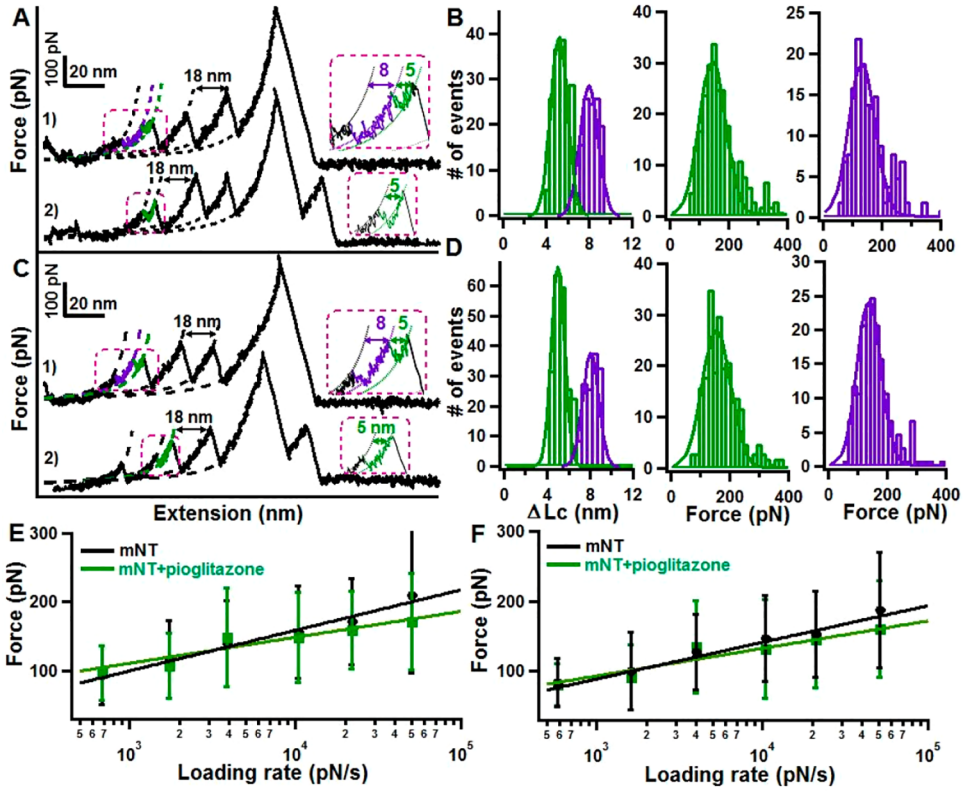


Figure 3. Different influences of pioglitazone binding on the 2Fe2S cluster and other parts. (A) Force−extension curves of the stepwise unfolding of mNT show the rupture event of the metal cluster (5 nm; green, enlarged in the box) and the unfolding event of mNT outside the cluster (8 nm; purple). (B) AFM results of the stepwise unfolding of mNT dimer including ΔLc histogram with two populations and corresponding force histogram. (C) Curves of the stepwise unfolding of mNT with pioglitazone binding. (D) AFM results of the stepwise unfolding of mNT dimer when pioglitazone is bound. (E and F) The linear relationship between the force and the logarithm of loading rate is used to obtain the kinetic stability of the metal cluster and protein.

which has been used to study the metal cluster in metalloprotein systems, to study mNT.[33−40]

Previously, the unfolding mechanism of mNT monomer was studied by AFM using a polyprotein construct, $(GB1)_3$-mNT-$(GB1)_3$.[9] Here, the well-characterized protein GB1 with a known contour length increment upon unfolding (ΔLc, 18 nm) and an unfolding force (*F*, 180 pN) is fused to mNT, serving as a single-molecule fingerprint and force caliper for reliable single-molecule detection and measurement.[41] However, we could not study the naturally occurring mNT homodimer because mNT in the polyprotein $(GB1)_3$-mNT-$(GB1)_3$ cannot dimerize.[42,43] We tried another often-used covalently linked-dimer strategy by connecting two mNT monomers in a single polyprotein as $(GB1)_3$-mNT-linker-mNT-$(GB1)_3$.[44−48] Unfortunately, only a small fraction of protein dimerized and underwent association−dissociation equilibrium demonstrated by the gel-filtration column (Figure S1). Thus, the mNT dimerization was inhibited by the adjacent protein or linker, possibly because of the steric hindrance, and the building of a functional mNT homodimer in a polyprotein form was challenging.

To solve this problem, we developed a new noncovalently bound strategy by dimerizing a GST-mNT monomer with a shorter, C-terminal protein-free mNT polyprotein Coh-$(GB1)_2$-mNT to minimize the steric hindrance. As a result, a polyprotein Coh-$(GB1)_2$-$[mNT]_2$ suitable for AFM-SMFS study and pioglitazone binding was obtained. The round bracket represents a covalent peptide bond linkage between protein units, and the square bracket represents a noncovalent protein−protein interaction between units. Consequently, the mechanism of pioglitazone's inhibition of the cluster transferability of mNT dimer was revealed by AFM measurement.

First, we constructed this noncovalently bound polyprotein Coh-$(GB1)_2$-$[mNT]_2$. We designed two different mNT monomers, one with His-tag and the other one with GST-tag (glutathione S-transferase) for sequential protein purification, and obtained the target protein (Figure 1B). First, a polyprotein $(His)_6$-Coh-$(GB1)_2$-mNT with an mNT monomer was constructed and purified by a Co-NTA resin column, yielding the monomer mostly (step 1; Figures S3C,D and S4). Then, a GST-mNT protein was constructed and purified by a GST-glutathione column, yielding both GST-mNT monomer and dimer (step 2; Figure S3C,E). Then, the two fractions were mixed. The small-sized GST-mNT monomer can bind the polyprotein, leading to the formation of target dimer, $(His)_6$-Coh-$(GB1)_2$-$[mNT]_2$-GST (step 3). The unreacted polyprotein $(His)_6$-Coh-$(GB1)_2$-mNT was eliminated by running through a GST-column. Finally, the GST tag was cleaved by PreScission protease, and the target protein dimer was purified and verified by a gel-filtration column (step 4, Figure 1B). The native PAGE gel experiment further indicated the mNT dimer formation.

To ensure an accurate measurement of mNT in different states, a site-specific and covalent protein attachment strategy for AFM system was used. This technical advance significantly improves the accuracy and efficiency of force spectroscopy

https://doi.org/10.1021/acs.jpclett.0c03852
J. Phys. Chem. Lett. 2021, 12, 3860−3867

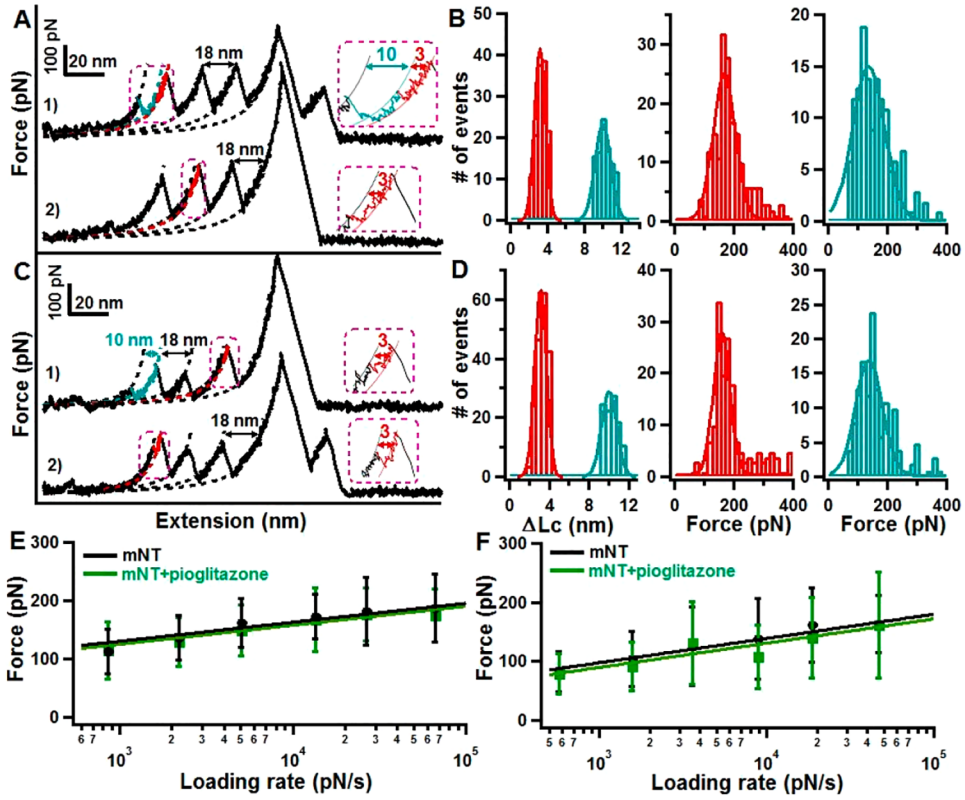


Figure 4. Moderate influence of pioglitazone binding on the partially ruptured $Fe_2S_2(Cys)_3$ intermediate. (A) Representative curves of the stepwise unfolding of mNT showing the rupture event of the partially ruptured metal cluster intermediate (3 nm; red) and the unfolding event of mNT outside the cluster (10 nm; cyan). (B) AFM results of the stepwise unfolding of mNT dimer including ΔLc histogram with two populations and corresponding unfolding/rupture force histogram. (C) Curves of rupture of 2Fe2S intermediate of mNT with pioglitazone binding. (D) AFM results of the stepwise unfolding of mNT dimer when pioglitazone is bound. (E and F) The linear relationship between the force and the logarithm of loading rate is used to obtain the kinetic stability of the $Fe_2S_2(Cys)_3$ and protein.

measurement (Figure 2A).[23,49,50] Briefly, the *Oa*AEP1-(C247A)-mediated enzymatic ligation method was used for protein immobilization, and the dockerin-cohesin [Doc-Coh] protein−protein interaction pair was applied as a reversible AFM pulling handle.[51,52] *Oa*AEP1 ligates two proteins/peptides between their N-terminal GL residues and C-terminal NGL residues. Thus, polyprotein Coh-$(GB1)_2$-$[mNT]_2$ with a C-terminal NGL can be covalently immobilized on a GL-functionalized glass coverslip by *Oa*AEP1 ligation. In addition, a GB1-Doc with an N-terminal GL can be linked to the NGL-functionalized AFM tip. Here, the peptide was previously coupled to the coverslip/cantilever by a heterobifunctional cross-linker reacting between the peptide and the amino-silanized surface (Supporting Information).[53]

Then, by pressing the GB1-Doc functionalized AFM tip onto the Coh-$(GB1)_2$-$[mNT]_2$ immobilized coverslip, a completely site-specifically conjugated construct, Tip-GB1-[Doc-Coh]-$(GB1)_2$-$[mNT]_2$-Glass, can be formed. When the tip was moved up vertically at a constant velocity (400 nm/s, here), mNT and GB1 were stretched and unfolded. Finally, the strongest [Coh-Doc] pair broke (>500 pN). Then, the tip moved to another place for repeated measurements on another polyprotein.

Next, we studied the binding effect of pioglitazone through the unfolding process of mNT dimer in the absence/presence of pioglitazone by single-molecule AFM. Stretching the polyprotein GB1-[Doc-Coh]-$(GB1)_2$-$[mNT]_2$ led to only a typical force−extension curve, including one force peak with a ΔLc of 13 nm from mNT unfolding, three peaks with ΔLc of 18 nm from GB1, and the last high force detachment peak from the dissociation of [Doc-Coh]. The ΔLc of the one-step unfolding of mNT was 12.7 ± 1.2 nm (fitted value ± 1 × sigma fit, n = 160, Figure 2B, yellow), similar to our previous AFM results for mNT monomer.[9] This agrees with the theoretical value from mNT unfolding leading to the extension of 37 amino acids (aa) between residues 68 to 104 (37 aa × 0.4 nm/aa − 0.46 nm = 14.3 nm, Figure 1A), in which a stable unfolding barrier exists. The unfolding force histogram is fitted by a Gaussian model (Figure 2C), yielding the force value of 120 ± 56 pN (fitted value ± 1 × sigma fit).[54]

Then, we performed the experiment in the presence of excess pioglitazone (~5000 times more, compared to the immobilized mNT). The 13 nm peak was observed again (12.6 ± 1.4 nm) but with a smaller force of 106 ± 59 pN (n = 137, Figure 2D,E). Moreover, we compared the unfolding kinetics of mNT with and without pioglitazone by pulling the protein under six different velocities. As expected for a two-state nonequilibrium process, the unfolding force of mNT was dependent on the logarithm of force loading rate and can be fitted by a linear line (Figure 2F). On the basis of the Bell−Evans model, the protein unfolding off rate (k_{off}) was 1.4 s^{-1} and 4.0 s^{-1} for the mNT and mNT−pioglitazone complex, respectively.[55,56] This demonstrated that the pioglitazone binding indeed affected mNT dimer and slightly weakened its stability.

https://doi.org/10.1021/acs.jpclett.0c03852
J. Phys. Chem. Lett. 2021, 12, 3860−3867

Besides the one-step unfolding, stepwise unfolding events of mNT dimer showing independent rupture event(s) of the 2Fe2S cluster were also observed by AFM-SMFS. This provides detailed information about the pioglitazone binding effects on the metal cluster. For example, a two-step unfolding event of mNT with a first 8 nm peak followed by a second 5 nm peak is shown in curve 1 of Figure 3A. Here, the first peak (in purple, 7.8 ± 1.2 nm, n = 158) was from the unfolding and extension of residues 68−72 and 88−104, which were outside the metal cluster (22 aa ×0.4 + 0.46 − 0.5 = 8.8 nm). Then, the second peak (in green, 5.0 ± 1.1 nm, n = 260) was from the rupture of the remaining 2Fe2S cluster, which led to the extension of residues 72−87 (15 aa × 0.4 − 0.5 = 5.5 nm). Their unfolding forces were 124 ± 64 pN and 137 ± 64 pN, respectively. Similarly, these two events (7.8 ± 1.0 nm, 130 ± 57 pN, n = 180; 4.8 ± 0.9 nm, 147 ± 68 pN, n = 233) can be observed when pioglitazone was bound (Figure 3C,D). Sometimes, only the 5 nm peak was observed (both curve 2 in panels A and C of Figure 3).

A major difference between mNT and mNT with pioglitazone was discovered when comparing their kinetic stability. The loading rate experiment showed that the k_{off} of the 5 nm peak for the metal cluster changed from 0.79 to 0.07 s^{-1}, a 10-fold decrease upon pioglitazone binding (Figure 3E). In addition, the Δx showed a considerable change from 0.16 to 0.25 nm. These results indicate that the effect of pioglitazone binding on mNT mainly targets the metal cluster and modifies its kinetic stability. Meanwhile, the kinetic parameter for the 8 nm peak from the protein structure outside the cluster changed moderately compared with the cluster. k_{off} changed from 0.89 to 0.25 s^{-1} with a 3-fold decrease, and the Δx changed from 0.18 and 0.24 nm (Figure 3F).

Besides the 5 nm peak from the one-step rupture of the intact metal cluster, a stepwise rupture of the cluster due to the labile Fe−N bond leading to a partially ruptured $Fe_2S_2(Cys)_3$ intermediate was also observed for mNT dimer. As shown in Figure 4A, a stepwise force peak was shown with a first 10 nm peak and a second 3 nm peak. Here, the 10 nm peak (10 ± 1.2 nm, n = 139, F = 129 ± 76 pN) was from the coupled unfolding of the protein outside the metal cluster (8 nm) and the rupture of the labile Fe−N bond (2 nm) in the cluster. Then, a second 3 nm force peak (3.0 ± 0.8 nm, n = 184, F = 160 ± 53 pN) was observed, which was from the rupture of the remaining $Fe_2S_2(Cys)_3$ cluster intermediate.

Nevertheless, their kinetic stability was less affected by the pioglitazone binding. First, their rupture/unfolding forces were similar (2.9 ± 0.8 nm, 152 ± 39 pN, n = 177; 9.8 ± 1.0 nm, 130 ± 64 pN, n = 141). Moreover, k_{off} for the 3 nm peak from the cluster rupture intermediate changed slightly from 0.007 to 0.01 s^{-1} (Figure 4E). Δx stayed at 0.29 nm. Compared with the pioglitazone binding effect on the intact metal cluster, these results indicate that the binding only slightly affects the intermediate. Similar results were observed for the 10 nm peak, which was mainly from the unfolding of the outside of the cluster. The k_{off} changed from 0.23 to 0.36 s^{-1}.

mNT is the first iron−sulfur protein identified as a drug target, which binds to type II diabetes TZD drug-like pioglitazone. Previous ensemble work showed that pioglitazone bound directly to the mNT homodimer and modulated its cluster transferability, in which the His87 was the key mediator. The primary purpose of this work was to study the molecular mechanism of the pioglitazone binding effect: why and how the pioglitazone binding affected the cluster transferability. Thus, we used AFM-SMFS to measure the unfolding mechanism and kinetic stability of mNT in the absence and presence of pioglitazone, and the construction of a polyprotein sample with naturally occurring mNT dimer ready for pioglitazone binding was the key. However, we found that mNT is difficult to dimerize when sandwiched by other proteins. Here, we developed a two-step method to build the target polyprotein based on a short polyprotein $(His)_6$-Coh-$(GB1)_2$-mNT. Then, a small GST-mNT can be dimerized, forming the target polyprotein after cleavage, $(His)_6$-Coh-$(GB1)_2$-$[mNT]_2$. Thus, a new strategy to obtain protein homodimer and other oligomers/complexes is demonstrated.

Next, we can characterize mNT in the homodimer form by AFM. First, it confirmed our previous work on mNT monomer. All three different types of unfolding pathways and force peaks of mNT were observed again in the dimer form. Besides the dominant one-step (13 nm) and two-step (8 + 5 nm, or 5 nm only, 10 + 3 nm, or 3 nm only) unfolding pathways, the three-step unfolding pathway (8 + 2 + 3 nm, 2 + 3 nm, Figure S5) with a low probability (0.5%) were detected. This verifies our previous peak assignment and explanation. Second, in agreement with ensemble studies, our single-molecule work also indicates that the pioglitazone binding affects the protein kinetics. Although to different degrees, all unfolding pathways are affected upon pioglitazone binding.

Perhaps the most important feature of our work is that the single-molecule AFM experiment distinguished the binding effect of pioglitazone on the different regions of mNT, especially from the two different stepwise unfolding scenarios (8 + 5 nm and 10 + 3 nm, Figure S5).[57] For the 8 + 5 nm pathway, the k_{off} of the protein outside the cluster (the 8 nm peak) changed relatively little (3-fold decrease) upon pioglitazone binding, while the k_{off} of the metal cluster (the 5 nm peak) changed significantly (10-fold decrease). This indicates that the pioglitazone mainly affects the properties of the $Fe_2S_2(Cys)_3(His)_1$ cluster by increasing its kinetic stability. This result agrees with previous ensemble studies both in vivo and in vitro, showing that the pioglitazone stabilizes the metal cluster and inhibits the metal cluster transfer.

For the 10 + 3 nm pathway, the k_{off} change of the partially ruptured $Fe_2S_2(Cys)_3$ cluster (the 3 nm peak) becomes much smaller (2-fold increase) when the Fe(III)−N(His87) bond is ruptured. In other words, when this bond is ruptured, the stabilizing effect of pioglitazone on the cluster largely disappears. Thus, the stabilizing effect of pioglitazone on the cluster is mainly through stabilizing the strength of this metal−ligand bond. Previous work showed the cluster-coordinating histidine 87 was the mediator for pioglitazone binding by monitoring the characteristic adsorption of the intact 2Fe2S cluster upon the cluster-transfer experiment. When this histidine is mutated to cysteine, the effect disappears. Here, our AFM results further nail down this mediator to the Fe(III)−N(His87) bond and support our previous hypothesis that this labile Fe−N bond and the partially ruptured $Fe_2S_2(Cys)_3$ cluster intermediate are involved with the release/transfer of the 2Fe2S cluster.

It is noted that a requirement is needed for building this noncovalently bound protein dimer/complex for SMFS measurement. Because of the immobilized nature of the target protein with a low concentration (Supporting Information), natural dissociated monomer from the polyprotein may not be able to rebind. Thus, the dissociation rate of the dimer should be low enough (<1 × 10^{-5}, $t_{1/2}$ = 19 h, for a first-order

https://doi.org/10.1021/acs.jpclett.0c03852
J. Phys. Chem. Lett. 2021, 12, 3860−3867

dissociation reaction) to allow reliable single-molecule characterization on a real dimer. The mNT studied here most likely fulfills this requirement. The two-monomer interexchange one β-strand to form the stable three-stranded β-sheet. Besides that, other interactions are present between the two monomers (Figure S6).[7] Indeed, the gel filtration of Coh-$(GB1)_2$-$[mNT]_2$ performed 48 h after GST-cleavage showed no residual mNT monomer dissociated (Figure S7). Moreover, we performed a control AFM experiment after one-day incubation of the immobilized sample. The relative frequency of different unfolding pathways for different samples and conditions were analyzed. AFM results showed that the ΔLc histogram was largely unchanged and suggested the designed noncovalently bound mNT dimer was stable over the period of (~12 h) measurement (Figure S8A,B and Table S1).

To prove this k_{off} requirement is necessary for our dimer construction method, we performed the AFM experiment in the presence of excess GST-mNT (1000 times). GST-mNT can self-dimerize partially, leading to free GST-mNT monomer in the solution. Although it binds to the Coh-$(GB1)_2$-mNT, it should bind much stronger with the natural mNT. Thus, it will compete the dissociated mNT and form the dimer GST-$[mNT]_2$ and push the dissociation reaction of Coh-$(GB1)_2$-$[mNT]_2$. Indeed, AFM experiments showed different results. The total frequency of unfolding events of 13, 10 + 3, and 8 + 5 nm decreased significantly from 75% to 64% (Figure S8C and Table S1). Finally, to obtain an accurate effect from pioglitazone by AFM-SMFS, pioglitazone binding should also fulfill the k_{off} requirement. Indeed, by adding only 10 times more pioglitazone, the frequency of different unfolding pathways changes (Figure S8D and Table S2). Here, the 3 nm peak is from the break of the partially ruptured metal cluster $Fe_2S_2(Cys)_3$, in which the Fe−N bond ruptured already. Less frequent observation of this peak indicates a more stable Fe−N bond. Its percentage is 7.5% (no pioglitazone), 7% (10 times), and 6.5% (5000 times). Unfortunately, there is no structural information about the mNT-pioglitazone complex currently. Most likely, two pioglitazone molecules bind to one mNT homodimer and may stabilize the dimer as well.

In this work, by constructing a polyprotein containing an mNT homodimer suitable for both single-molecule AFM measurement and pioglitazone binding, we show that pioglitazone binding may affect the metal cluster transferability of mNT by stabilizing the single, labile Fe(III)−N(His87) bond. Our work not only demonstrates the molecular mechanism of pioglitazone binding on mNT at a single-bond level but also provides an alternative method to build a protein complex for single-molecule studies.

■ ASSOCIATED CONTENT

Supporting Information

The Supporting Information is available free of charge at https://pubs.acs.org/doi/10.1021/acs.jpclett.0c03852.

Supplementary methods, note, figures, and tables (PDF)

■ AUTHOR INFORMATION

Corresponding Author

Peng Zheng − *State Key Laboratory of Coordination Chemistry, Chemistry and Biomedicine Innovation Center (ChemBIC), School of Chemistry and Chemical Engineering, Nanjing University, Nanjing, Jiangsu 210023, P.R. China;* orcid.org/0000-0003-4792-6364; Email: pengz@nju.edu.cn

Authors

Guobin Song − *State Key Laboratory of Coordination Chemistry, Chemistry and Biomedicine Innovation Center (ChemBIC), School of Chemistry and Chemical Engineering, Nanjing University, Nanjing, Jiangsu 210023, P.R. China*

Fang Tian − *State Key Laboratory of Coordination Chemistry, Chemistry and Biomedicine Innovation Center (ChemBIC), School of Chemistry and Chemical Engineering, Nanjing University, Nanjing, Jiangsu 210023, P.R. China*

Huaxing Liu − *State Key Laboratory of Coordination Chemistry, Chemistry and Biomedicine Innovation Center (ChemBIC), School of Chemistry and Chemical Engineering, Nanjing University, Nanjing, Jiangsu 210023, P.R. China*

Guoqiang Li − *State Key Laboratory of Coordination Chemistry, Chemistry and Biomedicine Innovation Center (ChemBIC), School of Chemistry and Chemical Engineering, Nanjing University, Nanjing, Jiangsu 210023, P.R. China*

Complete contact information is available at: https://pubs.acs.org/10.1021/acs.jpclett.0c03852

Notes

The authors declare no competing financial interest.

■ ACKNOWLEDGMENTS

This work was supported by the National Natural Science Foundation of China (Grant Nos. 21771103 and 21977047), the Fundamental Research Funds for the Central Universities (14380205), and by Natural Science Foundation of Jiangsu Province (Nos. BK20200058 and BK20202004). We are grateful to all members in the lab and appreciate the inspiring comments from anonymous reviewers.

■ REFERENCES

(1) Beinert, H.; Holm, R. H.; Münck, E. Iron-sulfur clusters: Nature's modular, multipurpose structures. *Science* **1997**, *277* (5326), 653−659.

(2) Johnson, D. C.; Dean, D. R.; Smith, A. D.; Johnson, M. K. Structure, function, and formation of biological iron-sulfur clusters. *Annu. Rev. Biochem.* **2005**, *74*, 247−81.

(3) Liu, J.; Chakraborty, S.; Hosseinzadeh, P.; Yu, Y.; Tian, S.; Petrik, I.; Bhagi, A.; Lu, Y. Metalloproteins containing cytochrome, iron-sulfur, or copper redox centers. *Chem. Rev.* **2014**, *114* (8), 4366−4469.

(4) Zuris, J. A.; Harir, Y.; Conlan, A. R.; Shvartsman, M.; Michaeli, D.; Tamir, S.; Paddock, M. L.; Onuchic, J. N.; Mittler, R.; Cabantchik, Z. I.; Jennings, P. A.; Nechushtai, R. Facile transfer of 2Fe-2S clusters from the diabetes drug target mitoNEET to an apo-acceptor protein. *Proc. Natl. Acad. Sci. U. S. A.* **2011**, *108* (32), 13047−13052.

(5) Takahashi, T.; Yamamoto, M.; Amikura, K.; Kato, K.; Serizawa, T.; Serizawa, K.; Akazawa, D.; Aoki, T.; Kawai, K.; Ogasawara, E.; Hayashi, J.-I.; Nakada, K.; Kainoh, M. A Novel MitoNEET Ligand, TT01001, Improves Diabetes and Ameliorates Mitochondrial Function in db/db Mice. *J. Pharmacol. Exp. Ther.* **2015**, *352* (2), 338−345.

(6) Conlan, A. R.; Paddock, M. L.; Homer, C.; Axelrod, H. L.; Cohen, A. E.; Abresch, E. C.; Zuris, J. A.; Nechushtai, R.; Jennings, P. A. Mutation of the His ligand in mitoNEET stabilizes the 2Fe-2S cluster despite conformational heterogeneity in the ligand environment. *Acta Crystallogr., Sect. D: Biol. Crystallogr.* **2011**, *67*, 516−523.

(7) Paddock, M. L.; Wiley, S. E.; Axelrod, H. L.; Cohen, A. E.; Roy, M.; Abresch, E. C.; Capraro, D.; Murphy, A. N.; Nechushtai, R.; Dixon, J. E.; Jennings, P. A. MitoNEET is a uniquely folded 2Fe-2S

outer mitochondrial membrane protein stabilized by pioglitazone. *Proc. Natl. Acad. Sci. U. S. A.* **2007**, *104* (36), 14342−14347.
(8) Tan, G.; Liu, D.; Pan, F.; Zhao, J.; Li, T.; Ma, Y.; Shen, B.; Lyu, J. His-87 ligand in mitoNEET is crucial for the transfer of iron sulfur clusters from mitochondria to cytosolic aconitase. *Biochem. Biophys. Res. Commun.* **2016**, *470* (1), 226−232.
(9) Song, G.; Ding, X.; Liu, H.; Yuan, G.; Tian, F.; Shi, S.; Yang, Y.; Li, G.; Zheng, P. Single-Molecule Force Spectroscopy Reveals that the Fe−N Bond Enables Multiple Rupture Pathways of the 2Fe2S Cluster in a MitoNEET Monomer. *Anal. Chem.* **2020**, *92* (21), 14783−14789.
(10) Hou, X.; Liu, R.; Ross, S.; Smart, E. J.; Zhu, H.; Gong, W. Crystallographic studies of human MitoNEET. *J. Biol. Chem.* **2007**, *282* (46), 33242−33246.
(11) Bieganski, R. M.; Yarmush, M. L. Novel ligands that target the mitochondrial membrane protein mitoNEET. *J. Mol. Graphics Modell.* **2011**, *29* (7), 965−973.
(12) Stigler, J.; Ziegler, F.; Gieseke, A.; Gebhardt, J. C. M.; Rief, M. The Complex Folding Network of Single Calmodulin Molecules. *Science* **2011**, *334* (6055), 512−516.
(13) Tapia-Rojo, R.; Eckels, E. C.; Fernández, J. M. Ephemeral states in protein folding under force captured with a magnetic tweezers design. *Proc. Natl. Acad. Sci. U. S. A.* **2019**, *116* (16), 7873−7878.
(14) Neupane, K.; Hoffer, N. Q.; Woodside, M. T. Testing Kinetic Identities Involving Transition-Path Properties Using Single-Molecule Folding Trajectories. *J. Phys. Chem. B* **2018**, *122* (49), 11095−11099.
(15) Alonso-Caballero, A.; Echelman, D. J.; Tapia-Rojo, R.; Haldar, S.; Eckels, E. C.; Fernandez, J. M. Protein folding modulates the chemical reactivity of a Gram-positive adhesin. *Nat. Chem.* **2021**, *13*, 172.
(16) Yu, H.; Siewny, M. G. W.; Edwards, D. T.; Sanders, A. W.; Perkins, T. T. Hidden dynamics in the unfolding of individual bacteriorhodopsin proteins. *Science* **2017**, *355* (6328), 945−950.
(17) Zhang, X.; Liu, C.; Wang, Z. Force spectroscopy of polymers: Studying on intramolecular and intermolecular interactions in single molecular level. *Polymer* **2008**, *49* (16), 3353−3361.
(18) Rief, M.; Gautel, M.; Oesterhelt, F.; Fernandez, J. M.; Gaub, H. E. Reversible unfolding of individual titin immunoglobulin domains by AFM. *Science* **1997**, *276* (5315), 1109−1112.
(19) Marszalek, P. E.; Lu, H.; Li, H.; Carrion-Vazquez, M.; Oberhauser, A. F.; Schulten, K.; Fernandez, J. M. Mechanical unfolding intermediates in titin modules. *Nature* **1999**, *402* (6757), 100−103.
(20) Schonfelder, J.; Alonso-Caballero, A.; De Sancho, D.; Perez-Jimenez, R. The life of proteins under mechanical force. *Chem. Soc. Rev.* **2018**, *47* (10), 3558−3573.
(21) Goktas, M.; Luo, C.; Sullan, R. M. A.; Bergues-Pupo, A. E.; Lipowsky, R.; Vila Verde, A.; Blank, K. G. Molecular mechanics of coiled coils loaded in the shear geometry. *Chem. Sci.* **2018**, *9* (20), 4610−4621.
(22) Hoffmann, T.; Tych, K. M.; Crosskey, T.; Schiffrin, B.; Brockwell, D. J.; Dougan, L. Rapid and Robust Polyprotein Production Facilitates Single-Molecule Mechanical Characterization of beta-Barrel Assembly Machinery Polypeptide Transport Associated Domains. *ACS Nano* **2015**, *9* (9), 8811−8821.
(23) Walder, R.; LeBlanc, M. A.; Van Patten, W. J.; Edwards, D. T.; Greenberg, J. A.; Adhikari, A.; Okoniewski, S. R.; Sullan, R. M. A.; Rabuka, D.; Sousa, M. C.; Perkins, T. T. Rapid Characterization of a Mechanically Labile alpha-Helical Protein Enabled by Efficient Site-Specific Bioconjugation. *J. Am. Chem. Soc.* **2017**, *139* (29), 9867−9875.
(24) Berkovich, R.; Fernandez, V. I.; Stirnemann, G.; Valle-Orero, J.; Fernández, J. M. Segmentation and the Entropic Elasticity of Modular Proteins. *J. Phys. Chem. Lett.* **2018**, *9* (16), 4707−4713.
(25) Moy, V. T.; Florin, E. L.; Gaub, H. E. Intermolecular Forces and Energies between Ligands and Receptors. *Science* **1994**, *266* (5183), 257−259.
(26) Conti, M.; Falini, G.; Samori, B. How strong is the coordination bond between a histidine tag and Ni-nitrilotriacetate? An experiment of mechanochemistry on single molecules. *Angew. Chem., Int. Ed.* **2000**, *39* (1), 215−218.
(27) Pill, M. F.; East, A. L. L.; Marx, D.; Beyer, M. K.; Clausen-Schaumann, H. Mechanical Activation Drastically Accelerates Amide Bond Hydrolysis, Matching Enzyme Activity. *Angew. Chem., Int. Ed.* **2019**, *58* (29), 9787−9790.
(28) Xing, H.; Li, Z.; Wang, W.; Liu, P.; Liu, J.; Song, Y.; Wu, Z. L.; Zhang, W.; Huang, F. Mechanochemistry of an Interlocked Poly[2]catenane: From Single Molecule to Bulk Gel. *CCS Chemistry* **2020**, *2* (1), 513−523.
(29) Popa, I.; Rivas-Pardo, J. A.; Eckels, E. C.; Echelman, D. J.; Badilla, C. L.; Valle-Orero, J.; Fernandez, J. M. A HaloTag Anchored Ruler for Week-Long Studies of Protein Dynamics. *J. Am. Chem. Soc.* **2016**, *138* (33), 10546−10553.
(30) Giganti, D.; Yan, K.; Badilla, C. L.; Fernandez, J. M.; Alegre-Cebollada, J. Disulfide isomerization reactions in titin immunoglobulin domains enable a mode of protein elasticity. *Nat. Commun.* **2018**, *9* (1), 185.
(31) Rico, F.; Russek, A.; Gonzalez, L.; Grubmuller, H.; Scheuring, S. Heterogeneous and rate-dependent streptavidin-biotin unbinding revealed by high-speed force spectroscopy and atomistic simulations. *Proc. Natl. Acad. Sci. U. S. A.* **2019**, *116* (14), 6594−6601.
(32) Bernardi, R. C.; Durner, E.; Schoeler, C.; Malinowska, K. H.; Carvalho, B. G.; Bayer, E. A.; Luthey-Schulten, Z.; Gaub, H. E.; Nash, M. A. Mechanisms of Nanonewton Mechanostability in a Protein Complex Revealed by Molecular Dynamics Simulations and Single-Molecule Force Spectroscopy. *J. Am. Chem. Soc.* **2019**, *141* (37), 14752−14763.
(33) Zheng, P.; Li, H. Highly Covalent Ferric-thiolate Bonds Exhibit Surprisingly Low Mechanical Stability. *J. Am. Chem. Soc.* **2011**, *133* (17), 6791−8.
(34) Beedle, A. E. M.; Lezamiz, A.; Stirnemann, G.; Garcia-Manyes, S. The mechanochemistry of copper reports on the directionality of unfolding in model cupredoxin proteins. *Nat. Commun.* **2015**, *6*, 7894.
(35) Lei, H.; Guo, Y. B.; Hu, X. D.; Hu, C. G.; Hu, X. T.; Li, H. B. Reversible Unfolding and Folding of the Metalloprotein Ferredoxin Revealed by Single-Molecule Atomic Force Microscopy. *J. Am. Chem. Soc.* **2017**, *139* (4), 1538−1544.
(36) Xia, J.; Zuo, J.; Li, H. Single molecule force spectroscopy reveals that the oxidation state of cobalt ions plays an important role in enhancing the mechanical stability of proteins. *Nanoscale* **2019**, *11* (42), 19791−19796.
(37) Perales-Calvo, J.; Lezamiz, A.; Garcia-Manyes, S. The Mechanochemistry of a Structural Zinc Finger. *J. Phys. Chem. Lett.* **2015**, *6* (17), 3335−3340.
(38) Arantes, G. M.; Field, M. J. Ferric-Thiolate Bond Dissociation Studied with Electronic Structure Calculations. *J. Phys. Chem. A* **2015**, *119* (39), 10084−10090.
(39) Zheng, P.; Arantes, G. M.; Field, M. J.; Li, H. Force-induced chemical reactions on the metal centre in a single metalloprotein molecule. *Nat. Commun.* **2015**, *6*, 7569.
(40) Yadav, A.; Paul, S.; Venkatramani, R.; Ainavarapu, S. R. K. Differences in the mechanical unfolding pathways of apo- and copper-bound azurins. *Sci. Rep.* **2018**, *8* (1), 1989−2001.
(41) Cao, Y.; Lam, C.; Wang, M.; Li, H. Nonmechanical Protein Can Have Significant Mechanical Stability. *Angew. Chem., Int. Ed.* **2006**, *45* (4), 642−645.
(42) Scholl, Z. N.; Yang, W.; Marszalek, P. E. Direct observation of multimer stabilization in the mechanical unfolding pathway of a protein undergoing oligomerization. *ACS Nano* **2015**, *9* (2), 1189−97.
(43) Kim, M.; Wang, C. C.; Benedetti, F.; Rabbi, M.; Bennett, V.; Marszalek, P. E. Nanomechanics of Streptavidin Hubs for Molecular Materials. *Adv. Mater.* **2011**, *23* (47), 5684−8.
(44) Bertz, M.; Buchner, J.; Rief, M. Mechanical Stability of the Antibody Domain CH3 Homodimer in Different Oxidation States. *J. Am. Chem. Soc.* **2013**, *135* (40), 15085−15091.

https://doi.org/10.1021/acs.jpclett.0c03852
J. Phys. Chem. Lett. 2021, 12, 3860−3867

(45) Kim, J.; Zhang, C.-Z.; Zhang, X.; Springer, T. A. A mechanically stabilized receptor−ligand flex-bond important in the vasculature. *Nature* **2010**, *466* (7309), 992−995.
(46) Zhang, X.; Rico, F.; Xu, A.; Moy, V. Atomic Force Microscopy of Protein-Protein Interactions. In *Handbook of Single-Molecule Biophysics*; Hinterdorfer, P., Oijen, A., Eds.; Springer US, 2009; pp 555−570.
(47) Milles, L. F.; Gaub, H. E. Is mechanical receptor ligand dissociation driven by unfolding or unbinding? *bioRxiv* **2019**, 593335.
(48) Wang, Y.; Barnett, S. F. H.; Le, S.; Guo, Z.; Zhong, X.; Kanchanawong, P.; Yan, J. Label-free Single-Molecule Quantification of Rapamycin-induced FKBP-FRB Dimerization for Direct Control of Cellular Mechanotransduction. *Nano Lett.* **2019**, *19* (10), 7514−7525.
(49) Ott, W.; Jobst, M. A.; Schoeler, C.; Gaub, H. E.; Nash, M. A. Single-molecule force spectroscopy on polyproteins and receptor−ligand complexes: The current toolbox. *J. Struct. Biol.* **2017**, *197* (1), 3−12.
(50) Zakeri, B.; Fierer, J. O.; Celik, E.; Chittock, E. C.; Schwarz-Linek, U.; Moy, V. T.; Howarth, M. Peptide tag forming a rapid covalent bond to a protein, through engineering a bacterial adhesin. *Proc. Natl. Acad. Sci. U. S. A.* **2012**, *109* (12), E690−E697.
(51) Ott, W.; Durner, E.; Gaub, H. E. Enzyme-Mediated, Site-Specific Protein Coupling Strategies for Surface-Based Binding Assays. *Angew. Chem., Int. Ed.* **2018**, *57* (39), 12666−12669.
(52) Yuan, G.; Liu, H.; Ma, Q.; Li, X.; Nie, J.; Zuo, J.; Zheng, P. Single-Molecule Force Spectroscopy Reveals that Iron-Ligand Bonds Modulate Proteins in Different Modes. *J. Phys. Chem. Lett.* **2019**, *10* (18), 5428−5433.
(53) Ebner, A.; Wildling, L.; Gruber, H. J. Functionalization of AFM Tips and Supports for Molecular Recognition Force Spectroscopy and Recognition Imaging. In *Atomic Force Microscopy: Methods and Protocols*; Santos, N. C., Carvalho, F. A., Eds.; Springer: New York, NY, 2019; pp 117−151.
(54) Ainavarapu, S. R. K.; Brujić, J.; Huang, H. H.; Wiita, A. P.; Lu, H.; Li, L.; Walther, K. A.; Carrion-Vazquez, M.; Li, H.; Fernandez, J. M. Contour Length and Refolding Rate of a Small Protein Controlled by Engineered Disulfide Bonds. *Biophys. J.* **2007**, *92* (1), 225−233.
(55) Evans, E.; Ritchie, K. Dynamic strength of molecular adhesion bonds. *Biophys. J.* **1997**, *72* (4), 1541−1555.
(56) Merkel, R.; Nassoy, P.; Leung, A.; Ritchie, K.; Evans, E. Energy landscapes of receptor-ligand bonds explored with dynamic force spectroscopy. *Nature* **1999**, *397* (6714), 50−3.
(57) Suren, T.; Rutz, D.; Mossmer, P.; Merkel, U.; Buchner, J.; Rief, M. Single-molecule force spectroscopy reveals folding steps associated with hormone binding and activation of the glucocorticoid receptor. *Proc. Natl. Acad. Sci. U. S. A.* **2018**, *115* (46), 11688−11693.

https://doi.org/10.1021/acs.jpclett.0c03852
J. Phys. Chem. Lett. 2021, 12, 3860−3867